Available online at www.sciencedirect.com
SCIENCE DIRECT®
Journal of Geodynamics 39 (2005) 444–460
JOURNAL OF GEODYNAMICS
http://www.elsevier.com/locate/jog

Estimation of the mass density contrasts and the 3D geometrical shape of the source bodies in the Yilgarn area, Eastern Goldfields, Western Australia

Gabriel Strykowski [a,*], Fabio Boschetti [b], Gábor Papp [c]

[a] *Danish National Space Center, Juliane Maries vej 30, 2100 Copenhagen, Denmark*
[b] *CSIRO, Division of Exploration and Mining, Australian Resources Research Centre, 26 Dick Perry Avenue, Kensington, WA 6151, Australia*
[c] *Geodetic and Geophysical Research Institute, Csatkai E. u 6-8, H-9400 Sopron, Hungary*

Accepted 18 April 2005

Abstract

We invert 2D surface gravity data constrained both by geological and seismic information. We use a number of pre-processing tools in order to reduce the general multi-body inversion into several single-body inversions, whereby we can reduce the overall complexity of the inversion task. This is done with as few assumptions as possible. Furthermore, for a single-body inversion we uncouple the determination of the shape of the causative sources from the determination of their mass density contrast to the surroundings. The inversion for the geometrical shape of the source body is done in steps. Firstly, a rough 3D shape of the source is modelled—a model consisting of the vertical mass columns of equal height. The horizontal extension is implied by the surface gravity signal. Subsequently, the shape of each source body is modified to obtain a better fit to the surface gravity data. In each modification step, the overall change of the shape of the source body is followed by an update of the mass density contrast to the surroundings. The technique was applied to a set of gravity data from the Eastern Goldfield area in Western Australia. The area has been widely studied in the past. In 1999, two seismic profiles that cross-sect the area were measured. Furthermore, an extensive geological modelling for the area has been conducted. The practical goal of this work was to verify the geological interpretation using the potential field data (mainly the gravity data although magnetic data were also available) and only weakly constrained by the seismic information. The result was the reconstruction of the 'rough' 3D geometry of the source bodies and the estimation of a constant mass density

* Corresponding author.
E-mail address: gs@spacecenter.dk (G. Strykowski).

0264-3707/$ – see front matter
doi:10.1016/j.jog.2005.04.004

contrast to the surroundings. A possible extension of this technique for detailed studies of the geological model is briefly discussed.

Keywords: Gravity; Seismics; Ambiguity; Explicit assumptions; Eastern Goldfields in Western Australia

1. Introduction

The well-known ambiguity in potential field analysis makes it necessary to use 'a priori' information in order to achieve meaningful interpretations of gravity or magnetic data. This 'a priori' information can take the form (in decreasing order of reliability) of geological observation, other types of geophysical data or mathematical constraints. Recent work (Strykowski, 1996) has shown that realistic mathematical constraints are necessary even in the presence of good geological/geophysical information. Today we still lack a satisfactory mathematical description of what makes a geological structure 'realistic'. Consequently, no general method to deal with the inversion of potential field data is currently available in the literature. In their handling of geological/geophysical data, the practitioners need to choose among a range of techniques with different level of flexibility, and, most importantly, with different underlying mathematical assumptions that necessarily determine the outcome of the inversion.

The work presented in this paper does not claim to solve the above inherent general problem of inverse potential field modelling. Rather it acknowledges it. What we propose could be described as a hybrid method between a standard geophysical potential field inversion and a geological type of forward modelling. The basic idea is to split the problem into a set of simple sub-problems where characteristics of the source geometry can be modelled robustly.

Under the favourable conditions of good seismic and geological constraints, as well as a reasonably simplified geology, we address the problem of reconstructing 3D underlying geology from gravity measurement. We do so by using a set of techniques recently developed by the authors to pre-process the data. Our aim is to reduce the computational effort and to limit the inherent ambiguity by turning a high dimensional multi-body inversion, into several separate lower dimensional single-body inversions.

We apply this method to a gravity data set from the Eastern Goldfields in Western Australia. The area had been previously studied via seismic survey and 1D gravity interpretation. We employ the available geological and seismic analysis as background information for the reconstruction of the 3D underlying geological structure from the 2D surface gravity image.

The area of Yilgarn Craton, Western Australia, located near the town of Kalgoorlie, is of great commercial interest as a major Australian gold province and classified as a world-class deposit. In recent years, Australian Geodynamics Cooperative Research Centre (AGCRC) – a consortium consisting of Australian Geological Survey Organisation (AGSO), CSIRO Division of Exploration and Mining, Monash University, LaTrobe University, Melbourne University and Compaq Computers Australia – was the main driving force in the intensive multi-disciplinary studies of the area. The work of AGCRC on Eastern Goldfields consisted of the reinterpretation of the 1991 regional AGSO deep seismic reflection traverse, followed by numerical modelling of this interpretation by CSIRO. This led private enterprises Placer and Fractal Graphics to develop exploration models. The main results of the first stage were presented

at the AGCRC Geodynamics and Gold Exploration in the Yilgarn Workshop in Perth, Western Australia (Wood, 1998). In the second phase, a grid of five deep seismic reflection lines through the area was acquired in August–September 1999. In the same field campaign detailed gravity measurements with a spacing of between 240 m and 320 m along the seismic profile were also acquired. The results of AGCRC Yilgarn Project were presented at Yilgarn Seismic Workshop in Kalgoorlie (Goleby et al., 2000). The workshop also included other work done in the area on the gravity and magnetic modelling, the high-resolution seismic work by Kalgoorlie Consolidated Gold Mines, the geological overviews by the Geological Survey of Western Australia, and the industry sponsored studies on the metamorphic grade.

2. Methods

A combination of different methods that we recommend for potential field inversion can be summarised as follows:

(1) We isolate the main anomalies in the gravity image (residual/regional separation). In doing so we account for the gravitational effect of the adjacent sources (inclusive the background) on each anomaly. Subsequently, we proceed in analysing each isolated anomaly separately.
(2) We propose a multi-scale edge based technique to determine the correct local gravitational zero level for our inversion.
(3) Similarly, we propose another multi-scale edge based technique to determine the depth-to-the-top of the anomalies.
(4) As a preparation for the inversion we first build the initial 3D model of the source geometry. One source model for each isolated anomaly. We describe in some details the criteria for choosing the optimal initial model. In particular, we discuss how to decouple the estimation of the source geometry from the estimation of the mass density contrast.
(5) In the inversion, the initial rough 3D source model is modified in the horizontal to obtain a better fit of the gravitational response of the model to the associated isolated surface gravity anomaly. The geometry of the source body is changed gradually and the constant mass density contrast between the source model and the surroundings is updated.

In general, even though not all of the above methods were equally important for the practical modelling task for the Yilgarn area in Western Australia, we mention them, nevertheless, for the sake of completeness, and because they fit into our philosophy of hierarchical robust modelling with few, explicit and meaningful assumptions. We believe that a combination of the surface gravity information and seismic information implies which source characteristics can be modelled robustly. Thus, the choice of the adequate methods of modelling can vary from case to case. In the case of potential field modelling in Yilgarn area of Western Australia, we turn a general multiple body inversion into three separate single-body inversions. For each of the above single-body inversions, we assume a constant mass density contrast to the surroundings. It means that the source geometry can be modelled separately, i.e. we can disregard the mass density factor. This procedure results in both algorithmic and computational advantages. We now describe each of the above methods separately.

2.1. Anomaly isolation

In a recent work we have explored the isolation of the gravity anomalies on 1D profiles. The technique does not merely separate the anomalies, but also, importantly, removes the gravitational effect of the adjacent sources and the background. The full description of the technique, as well as a discussion of the underlying assumptions can be found in Boschetti et al. (2004). Here we briefly summarise the algorithm with the help of Fig. 1.

Let us suppose we want to remove the leftmost feature (the local maximum) of the signal (see Fig. 1a). The first step is to approximate the main feature of the signal as if the left feature was not present (Fig. 1b). Modelling the centre anomaly using simple elementary sources does this. Subsequently, we can subtract this approximation from the original signal (Fig. 1c).

The second step is to approximate the isolated left feature on the whole length of the original profile (Fig. 1d) using elementary sources and to subtract this approximation from the original signal (Fig. 1e). By iterating the first and the second step we achieve a further reduction of the effect of each anomaly on one another and we quickly reach convergence, i.e. when further iterations do not alter the relevant parts of the profiles shown in Fig. 1b and e. The above publication demonstrates that the quality of the proposed reconstruction is quite satisfactory.

The generalisation of the above technique to 2D images is not straightforward, mostly because it is more difficult to accurately establish the borders of the individual anomalies in certain circumstances.

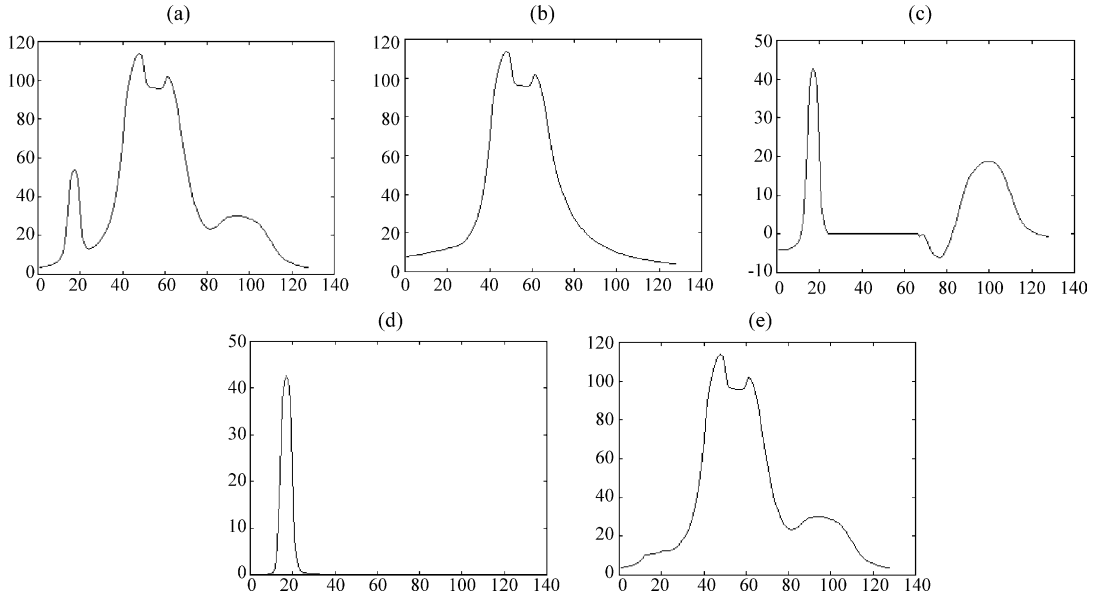

Fig. 1. Explaining the anomaly isolation algorithm in 1D. (a) The original profile; (b) step 1: the main anomaly is modelled using elementary sources; (c) the difference between the original profile and the model of the main anomaly; (d) step 2: the lateral continuation of the left anomaly along the whole profile is modelled using elementary sources; (e) the difference between the original profile and the model of the left anomaly. Steps 1 and 2 is repeated until the convergence is reached, i.e. the profiles shown on (b) and (e) does not differ is the vicinity of the left anomaly.

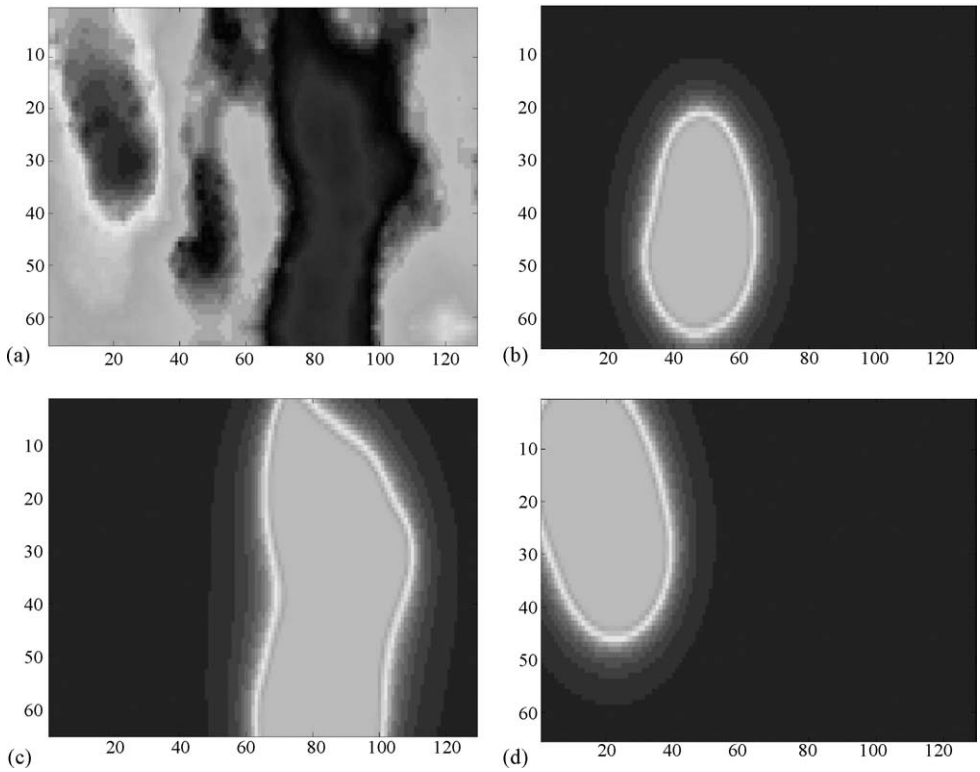

Fig. 2. Explaining the anomaly isolation algorithm in 2D. The frames mark the approximate location of the source of the identified anomalies to be isolated. (a) The original gravity image for the Yilgarn area, Western Australia; (b) a frame for anomaly 1, the central positive anomaly; (c) a frame for anomaly 2, the large positive anomaly; (d) a frame for anomaly 3, the negative north-western anomaly.

We employed a simplification that in addition makes the algorithm computationally very fast. In the following, we use the term gravity image as a synonym for the gravity anomaly given on a regular grid. The advocated technique bears some resemblance to image processing. The grid points are synonymous to the pixels of the image and the grid values to the pixel values.

We use isolines of the gravity image to roughly approximate the horizontal location of the causative source for each anomaly. This is shown in Fig. 2. The original gravity image is shown in Fig. 2a. Fig. 2b shows the approximate horizontal position of the material that generates the small positive anomaly in the centre. Fig. 2c and d show, respectively, the areas corresponding to the large positive anomaly and to the negative anomaly. In the following, we will call such marking of the approximate location of the source for a given anomaly as frames.

The frames have value 1 for grid points in correspondence with the location of the source and 0 elsewhere with a smooth transition at the border. Also, a cosine bell tapering has been used at the edge of the whole area to facilitate subsequent Fourier-domain based analysis. Each frame has its complementary frame, i.e. the value is 0 in correspondence of the location of the source of the anomaly and 1 elsewhere with a smooth transition at the edge.

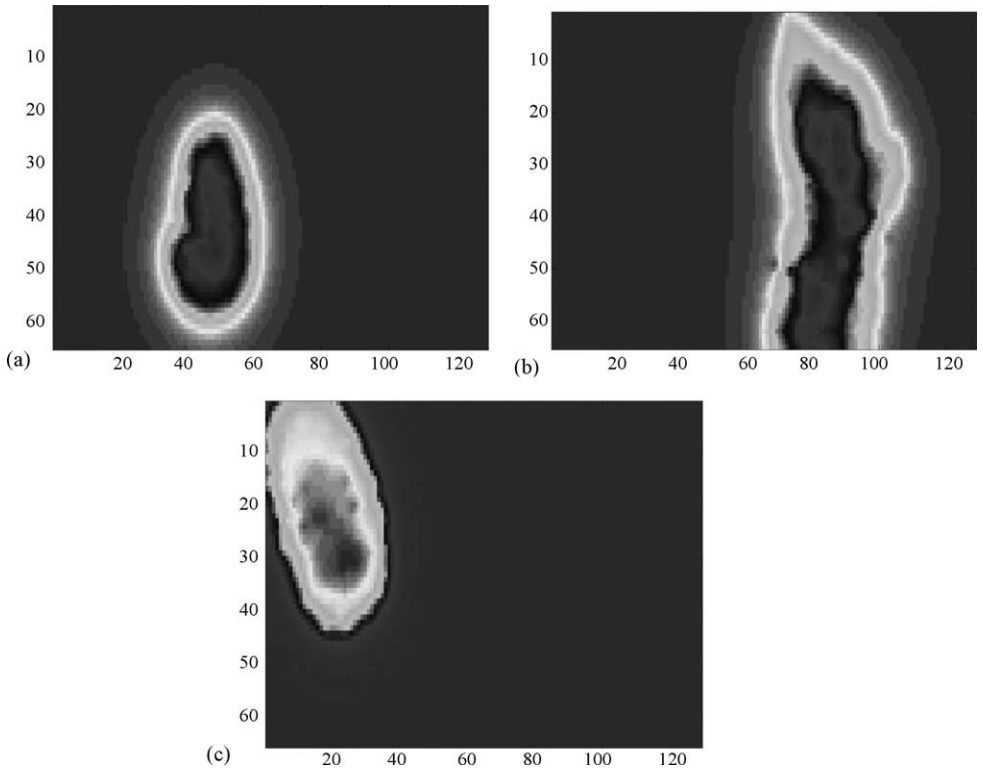

Fig. 3. The result of the 2D anomaly separation for the study area—the Yilgarn area of Western Australia. (a) The gravity image corresponding to the isolated small positive gravity anomaly (anomaly 1); (b) the gravity image corresponding to the isolated large positive anomaly in the centre of the area (anomaly 2); (c) the isolated gravity image for the isolated north-western negative anomaly (anomaly 3).

The anomaly isolation in 2D proceeds as follows:

1. We apply harmonic downward continuation to the original gravity image.
2. We multiply pixel-wise the downward continued gravity image by the complementary frame (see above) for each of the three frames. This corresponds to removing the gravity effect of the causative source for each anomaly from the downward continued gravity image.
3. We apply harmonic upward continuation for each of the three images obtained in 2. Conceptually, we model the gravity image of the background for each anomaly.
4. We remove the effect of the adjacent features from each anomaly by subtracting the upward continued images from the original map. We obtain three images each containing only one anomaly.

As with the 1D technique the method converges within a few iterations. Clearly, the downward continued image does not correspond to any physical source. However, we treat them merely as ‘equivalent layer sources’ able to approximate the gravity field under analysis for the sole purpose of isolating the anomalies. The reconstruction of physically realistic sources will be the goal of the final inversion. The result of the separation is shown in Fig. 3.

2.2. Evaluation of the regional gravity level

Visual inspection of the gravity image does not suggest the presence of a noticeable regional trend. Nevertheless, some pre-processing is necessary before attempting any numerical inversion, in order to establish the local gravity zero level. This determines the amplitude of the anomalies and eventually affects the reconstruction of causative sources. Even using Fourier methods, mostly insensitive to constant shifts, the proper accounting of the zero level is significant since it affects the way the cosine bell is designed in order to reduce border effects.

In another recent work (Poulet et al., 2001), it has been proposed that the use of multiscale edges can help identifying such zero level. For a detailed description of multiscale edge theory applied to potential field data we refer to (Hornby et al., 1999). The technique is based on the following concept: given a gravity signal, we can calculate the location of the edges of such signal (i.e. the locations at which the gradient of the signal is locally maximum in absolute value). In general, these edges change position as a function of the height at which the signal is measured. An example, for a block shaped source, is shown in Fig. 4.

The edges caused by a point source in 1D generate two symmetrical lines. For 2D signal they generate a cone (Hornby et al., 1999). Furthermore, the slope of such lines or cone is fixed. For 1D signals this slope is $1/\sqrt{3}$, and for 2D signals it is 1/2.

Thus, at a sufficient level above a source of finite size, the gravitational signal behaves like a point source and the edges of the source gravity response align with the slopes of the point mass gravity response. If the zero level of the isolated anomaly is wrong, the total gravity signal might also contain a signal due to some additional source, possibly of non-finite size (compared to the extension of the signal). In this case, the edges of the upward continued image may not align with the edges of the point mass image or may align with the incorrect slope. This is valid both for the profile data and for the 2D data. The anomalies in Fig. 3 have been checked for the correct regional zero level by projecting the upward continued 2D gravity images on 1D profiles. The choice of the correct zero level is done by trail and error technique.

One remark concerning the correct zero level in relation to the method of inversion proposed in this paper is that the mean value of the gravity image is subtracted prior to the inversion. Thus, it seems

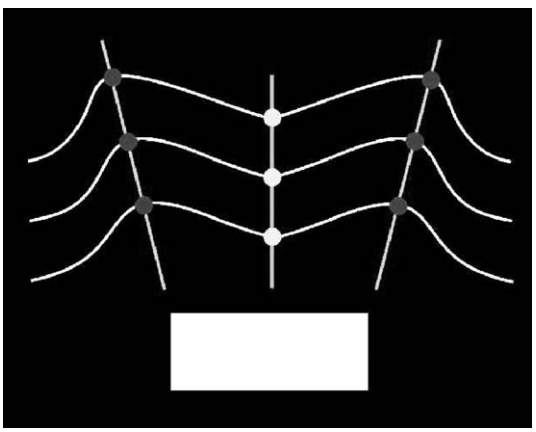

Fig. 4. Multiscale edges due to the gravity response of a rectangular source. At different levels of upward continuation the location of the edges (dark dots) are shown. The white dots show the location of the maximum of the anomaly at each level.

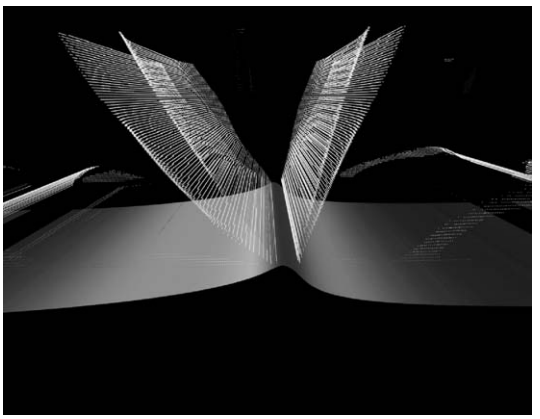

Fig. 5. Multiscale edges from 1st VD signal (inner edges) and standard gravity signal for an inclined dyke. They two sets of edges converge at a vertical level corresponding to the top of the source.

that the careful estimation of the zero level is not used in the subsequent modelling. Nevertheless, the above remark about the adequate cosine-bell tapering is valid, and the residual/regional separation via Fourier-domain (as described above) makes the estimation of the correct zero-level worthwhile.

2.3. Visual estimation of depth-to-the-top of sources

The geological interpretation described in the previous section suggests that the main anomalous bodies outcrop, or at least are characterised by a very shallow depth to the top. This information is very important, since fixing the top of the source reduces the ambiguity of the source model.

Here we propose the use of a semi-quantitative tool to obtain a visual appraisal of the depth-to-the-top of the causative sources and possibly verify such assumption. This idea is also based on the use of multiscale edges.

For this purpose we use two sets of multiscale edges. One set is represented by the standard edges as introduced in the previous section. The second set consists in the edges generated by the first vertical (1st VD) derivative of the same signal (i.e. the vertical gravity gradient). The two sets of edges are visualized in 3D (see Fig. 5), for a gravity signal due to an inclined, outcropping dyke.

As seen in Fig. 5, the edges detected on the standard gravity image and the edges due to the 1st VD image behave differently at different levels of upward continuation. This is due to the fact that the 1st VD signal is ‘sharper’ than the gravity, i.e. the 1st VD edges have a steeper slope or stay ‘closer’ to the source location. At the top of source both the gravity signal and its 1st VD become maximally sharp. We can use this feature to obtain a visual estimate of the depth-to-the-top. In Fig. 5, we see that both sets of edges meet over the gravity surface, where the dyke outcrops.

We employed the same idea to analyze the gravity profiles over the three anomalies under investigation to verify whether the assumption of very shallow or outcropping sources is correct. As an example, we show the profile over the smaller positive anomaly in the centre of the surveyed area. Fig. 6 shows both the standard edges and the 1st VD edges. As we can see the edges converge towards the same location just at the measurement level. We are thus encouraged to accept the geological interpretation suggesting outcropping causative sources.

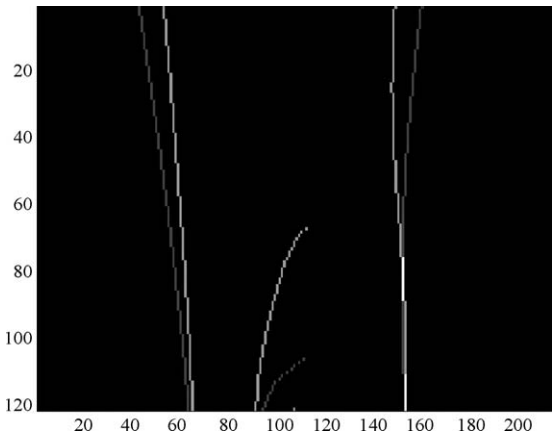

Fig. 6. Gravity edges and 1st VD edges for the main positive anomaly projected on a gravity profile. The edges meet at the measurement level (the surface), suggesting the presence of a very shallow source.

2.4. Preparation for the inversion

Fig. 3 shows the isolated gravity anomalies for the Yilgarn area in Western Australia. Up to this point, the only relation to the source model was its implicit horizontal location, which was used in the 2D regional/residual separation (cf. the notion of frames in Fig. 2). Next, we assume that each of the three isolated anomalies was generated by a finite source. This assumption is supported by the seismograms from the area. The gravity and magnetic interpretation of five profiles from the Yilgarn Project (Goleby et al., 2000) yields a complicated pattern of contrasting geological units. In particular, the profiles 2 and 5 that cross-sect the chosen sub-area show a co-location between the isolated anomalies in Fig. 2 and certain geological units (see Table 1). Furthermore, these sources are shallow (in fact outcropping). One

Table 1
The results

	Anomaly 1	Anomaly 2	Anomaly 3
Isolated anomaly: Δg_{ext} (m/s^2)	8.9×10^{-5}	25.2×10^{-5}	-25.7×10^{-5}
$\Delta g/\Delta g_{ext}$, isoline used	0.4	0.4	0.4
Height of mass columns (m)	5000	4000	4500
Initial $\Delta\rho$ (kg/m^3)	72	202	−185
Final $\Delta\rho$ (kg/m^3)	75	207	−189
Number of iterations	12	39	10
Source rock (Goleby et al., 2000)	Lower basalt/komatite	Upper basalt	Granitoids
Laboratory values of mass density ρ (Goleby et al., 2000) (kg/m^3)	2710–3050	2710–3010	2500–2650
Seismic profiles (Goleby et al., 2000)	Profile #2 and 5 cross each other just west of the anomaly	Profile #2 cross-sects the central edge and profile #5 cross-sects the southern edge of the anomaly	Profile #2 is located just south of the anomaly
Depth to the base on seismic profiles (Goleby et al., 2000) (m)	5000	3500	1000–2500

assumption for further modelling is that each of the three isolated sources has a constant mass density contrast to the surroundings. This is in general not always the case and such assumption has of course implications for the geometry of the source model. Nevertheless, the first goal of the inversion is to place the source model correctly in the subsurface and to determine roughly its geometry. The model can subsequently be modified reflecting the independent information, e.g. the seismograms.

The assumption of a constant mass density contrast to the surroundings has an important advantage, which is the decoupling of the source strength (the mass density contrast) and the source geometry. Consider the Newton's integral relating the surface gravity signal Δg and the source strength (i.e. the mass density contrast) $\Delta\rho$:

$$\Delta g = \int_{\Omega} \Delta\rho G_{\Delta g}\, \mathrm{d}\Omega \tag{1a}$$

where $G_{\Delta g}$ is the (Newtonian) kernel function for and Ω is the integration domain.

Clearly, if $\Delta\rho$ is constant we have:

$$\Delta g = \Delta\rho \int_{\Omega} G_{\Delta g}\, \mathrm{d}\Omega \tag{1b}$$

i.e. the source strength $\Delta\rho$ can be viewed as a scaling factor and the geometry of the anomalous gravitational signal is the integral on the right hand side of Eq. (1b).

Eq. (1b) can be used to decouple the source strength and the effect of geometry from in the isolated gravity anomalies shown in Fig. 3. The goal is to construct the initial model of the source geometry. We assume that the horizontal extension of the source is somehow reflected in the shape and in the location of the isolines of the corresponding gravity signal. The question is which isoline should be used?

Before answering this question we found it convenient to transform the three isolated gravity anomalies to a normalized form. The isolated anomalies were first centred, i.e. we have subtracted a mean value from each of the three isolated gravity grids. In the following, Δg denotes the centred isolated anomaly, i.e. the mean value over the whole area for each anomaly is zero. The reason for this is somehow technical. Briefly, the mean gravity value over the whole area includes the gravitational effect of other sources than the studied source. Furthermore, this constant mean value is arbitrary with regard to the parametrization of the subsurface. In other words, we cannot be sure that the mean value of gravity signal is really generated from depths covered by the Earth's model (which of course is limited in depth). Thus, if not accounted for, we risk the inconsistency between the parametrization and the surface signal. Such inconsistency can bias the result of inversion.

Secondly, we have scaled the surface signal by the extreme value $\Delta g_{\mathrm{ext}} = \mathrm{sign}(\Delta g_k) \times \max\{|\Delta g_k|\}$, where k is the index for the finite number of the surface gravity grid points. Subsequently, the gravity grids for the isolated anomalies can be normalized:

$$\frac{\Delta g}{\Delta g_{\mathrm{ext}}} = \frac{\Delta\rho}{\Delta g_{\mathrm{ext}}} \int_{\Omega} G_{\Delta g}\, \mathrm{d}\Omega \tag{2a}$$

Notice that the grid values of the normalized signal lie in the interval]–1,1].

Eq. (2a) can be expressed even more conveniently by introducing the notion of unit mass density $\Delta\rho_{\mathrm{unit}}$, where $\Delta\rho_{\mathrm{unit}} = 1000\,\mathrm{kg/m^3}$ (corresponding to $1\,\mathrm{g/cm^3}$).

$$\frac{\Delta g}{\Delta g_{\mathrm{ext}}} = \frac{\Delta\rho}{\Delta\rho_{\mathrm{unit}}} \frac{\Delta g_{\mathrm{unit}}}{\Delta g_{\mathrm{ext}}} \tag{2b}$$

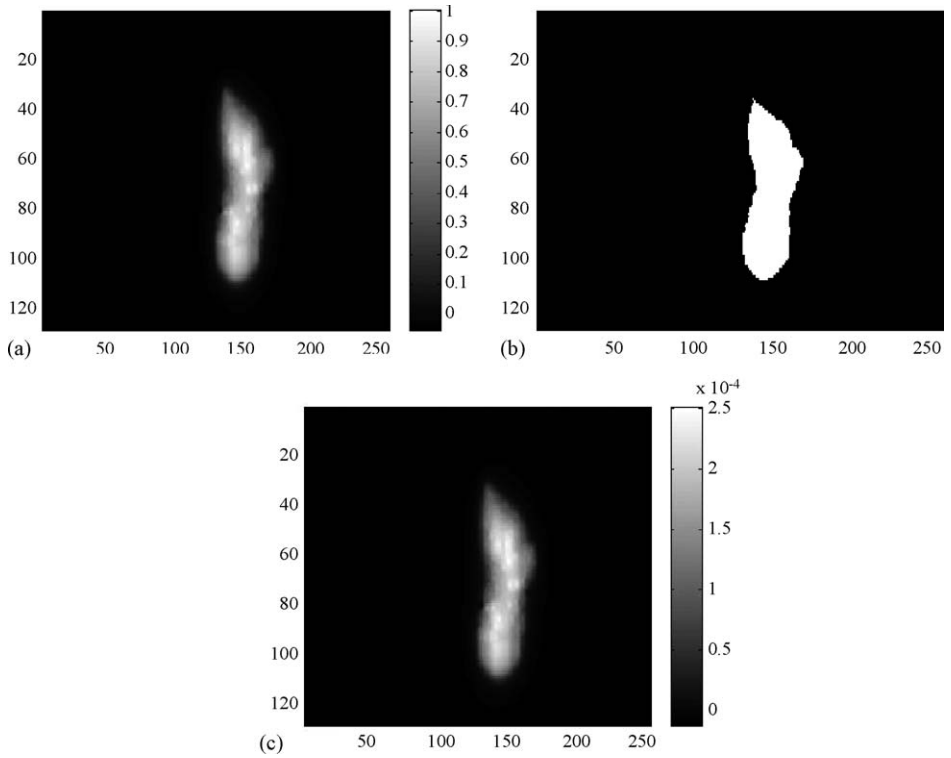

Fig. 7. Illustrating the construction of the initial source model for anomaly 2. (a) The normalized isolated gravity image $\Delta g/\Delta g_{\text{ext}}$; (b) the isoline 0.4 on (a) is used to obtain the horizontal location of the source. In the vertical, the source model thickness is 4 km. (c) Gravitational response Δg_{unit} (unit m/s^2) of the source model.

where $\Delta g_{\text{unit}} \equiv \Delta\rho_{\text{unit}} \int_{\Omega} G_{\Delta g}\, \mathrm{d}\Omega$. The advantage of this Eq. (2b) is that we get rid of physical units on the left and right hand side of the equation. The gravitational response of the Earth model Δg_{unit} is computed for unit mass density $\Delta\rho_{\text{unit}}$, scaled by Δg_{ext} and related to the left hand side of Eq. (2b) by $\Delta\rho/\Delta\rho_{\text{unit}}$, which is a unitless quantity. Furthermore, the unitless quantities $\Delta\rho/\Delta\rho_{\text{unit}}$ and $\Delta g_{\text{unit}}/\Delta g_{\text{ext}}$ on the right hand side of Eq. (2b) express, respectively, the source strength of the finite source body and its geometry.

Retuning to the question of which isoline one should use to obtain the initial source model, Fig. 7 illustrates the principles for the construction of such model. Fig. 7a shows the normalized isolated anomaly $\Delta g_{\text{unit}}/\Delta g_{\text{ext}}$. (Notice that the area has been extended as compared to Fig. 3 to avoid the edge effects.) Fig. 7b shows how the isoline 0.4 has been used to yield the initial horizontal extension of the source. As mentioned above, seismic evidence indicates that the top of the source outcrops. We have adopted a simple source model in which the homogenous, rectangular vertical prisms are located horizontally as indicated by Fig. 7b. The top of the prisms is at the surface and the base in some constant depth. Fig. 7c shows Δg_{unit} for the initial source model for a base at a depth of 4 km.

Choosing the best initial source model starts with the collection and the assessment of the independent information, such as: the thickness of the cross-section of the source rock along the seismic profiles, the geophysical information about the average mass density of the possible source. One should keep in

mind that the depth-conversion of seismograms is not perfect, and that the average thickness and the depth of burial of some geological unit on seismograms may deviate away from the seismic profile. Thus, it is more correct to regard the geometrical information from seismograms as a guideline rather than as fixed information. In practise, a number of candidate initial models were tested using few isolines of the normalized gravitational signal and few different depths to the base of the mass columns. For each combination of these two discrete model parameters (the isoline value and the height of the mass columns) Δg_{unit} was computed. Using Eq. (2b), each Δg_{unit} this model was scaled to yield the best possible approximation to Δg. Notice, that it means that the mass density contrast $\Delta\rho$ was estimated. The condition was that the two gravity signals should be equal for the location of the grid point where we have the extreme value Δg_{ext}.

Thus, denoting the position of such grid point as x_k the condition for the estimation of the initial mass density contrast is:

$$\Delta\rho = \frac{\Delta g(x_k)}{\Delta g_{\text{unit}}(x_k)} \Delta\rho_{\text{unit}} \tag{3}$$

Subsequently, Δg can be compared to $\Delta\rho \times \Delta g_{\text{unit}}$ over the whole area to yield the misfit statistics. In addition, the value of $\Delta\rho$ can be compared to what is known about the physical properties for this particular geological unit. Also, the misfit figure can be studied for systematics. The answer to which initial model is the best is by no means easy. By inspecting all the above pieces of information the best initial model of the source geometry and the corresponding estimate of the initial mass density contrast can be found.

2.5. The inversion

The technique used here is basically the one proposed by Strykowski (1999). It is not a standard geophysical inversion method. It can be classified as a hybrid method of geological forward modelling (in 3D) enhanced by the robust estimation of certain model parameters by least squares fit of 'the measured' to 'the modelled'. Conceptually, the main issue is the correct weighting of the information contained in the data and the use of the mathematical assumptions which are necessary to obtain a unique source model. The nature of the potential field inverse problems is such that one easily can 'overdo' the mathematics, i.e. to bridge the inherent non-uniqueness of the potential field problems merely by the mathematical assumptions. Such assumptions are not necessarily related to the true distribution of sources, and theirs impact on the constructed Earth's model is sometimes unclear (e.g. Strykowski and Boschetti, 2003). The obtained model can be inadequate to approximate the true distribution of sources even with the correct input information and, which is worse, without being contradicted by the available information. The modelling philosophy that we advocate is to downgrade the mathematical assumptions (i.e. to use them only if absolutely necessary) and to put emphasis on the 'common sense' explicit geological assumptions. Geologists think in terms of 'structures'—the type of information, which is often difficult to formalise mathematically, but which, nevertheless, is a direct and a plausible guess of how the geophysical sources in the subsurface are distributed than what can be achieved by any mathematical constraint.

In the construction of the initial model (see above) the source model has already been placed approximately correctly in the subsurface. Conceptually, we think of this initial source model as a blurred image of a more correct source model—a model, which can be obtained by the modification of the initial one. As argued above, such modification should not be based on mathematical assumptions, but rather reflect

the explicit geological assumptions. The initial model is rather 'stiff', i.e. it cannot resolve the details in the gravity signal. It merely models the average properties of the source using a simplified parameter space. In this sense, the main idea can be traced back to the method of Backhus and Gilbert of robust estimation of the averages of the unknown source functions, which can be uniquely determined by the data (see e.g. Jackson, 1979).

Our explicit geological assumption for the source model modification is that it can be improved by a gradual change of the horizontal extension. Firstly, the periphery of the initial source model is identified, i.e. the location of the mass columns at the edge of the source model. A computer program visits all periphery mass columns sequentially and 'clockwise'. For each mass prism it is investigated whether the removal of the prism will improve the fit between Δg and $\Delta\rho \times \Delta g_{\text{unit}}$?

In practice, a master unit-mass-density gravity response of the vertical mass column is computed in a surface grid with the same spacing as the gravity grid Δg (see Nagy et al., 2000). Subsequently, this master gravity response is centred by removing the mean value.

In order to remove the gravity effect of a certain mass column along the periphery, the master vertical-mass-column gravity response is multiplied by $\Delta\rho$ and subtracted from $\Delta\rho \times \Delta g_{\text{unit}}$. The master gravity response is centred on the location of the associated periphery grid point. Once the computer program has made a full cycle along the periphery, a new modified model of the source gometry has been created. The gravitational response of this model has also changed, and a new updated value of the mass density contrast can be computed by Eq. (3). The proposed stepwise procedure converges in a sense that at some stage the removal of more mass columns will not improve the gravity fit. A full cycle followed by an update of the mass density value is here called the iteration even though the technique is clearly different from the standard gradient methods of the non-linear geophysical inversion. Fig. 8 illustrates the inversion procedure.

3. Results and discussion

In the previous section, the proposed methods for robust potential field modelling were described in some details. In this section, the results obtained for the Yilgarn area in Western Australia using the above techniques will be briefly discussed. In our modelling the main source of information were: the regional AGCRC gravity data, the detailed gravity data along profiles 2 and 5, and the publication (Goleby et al., 2000). The publication contains geological interpretation of both profiles based on seismics and the detailed information about the mass density values for certain identified geological units.

It is relevant to emphasize that our modelling is not directly based on the above publication except for the use of the same regional gravity data. Neither the detailed gravity data along the profiles were used. Rather, the detailed information in (Goleby et al., 2000) was used as a guide for making geological assumptions. Our contribution was to extend the model from profile models to 3D models for three selected sources. Table 1 summarises the obtained results.

One obvious test of the results was to project the source model before and after the inversion onto profiles 2 and 5 and to inspect whether the source model cross-section after the inversion is a better approximation to the seismic interpretation than the corresponding cross-section of the initial model. The source model for anomaly 1, which is cross-sected by both profiles (see Table 1), behave exactly this way. However, this result should not be seen as anything else but as an indication that the proposed inversion technique works correctly. One should not expect the results of seismic interpretation and the

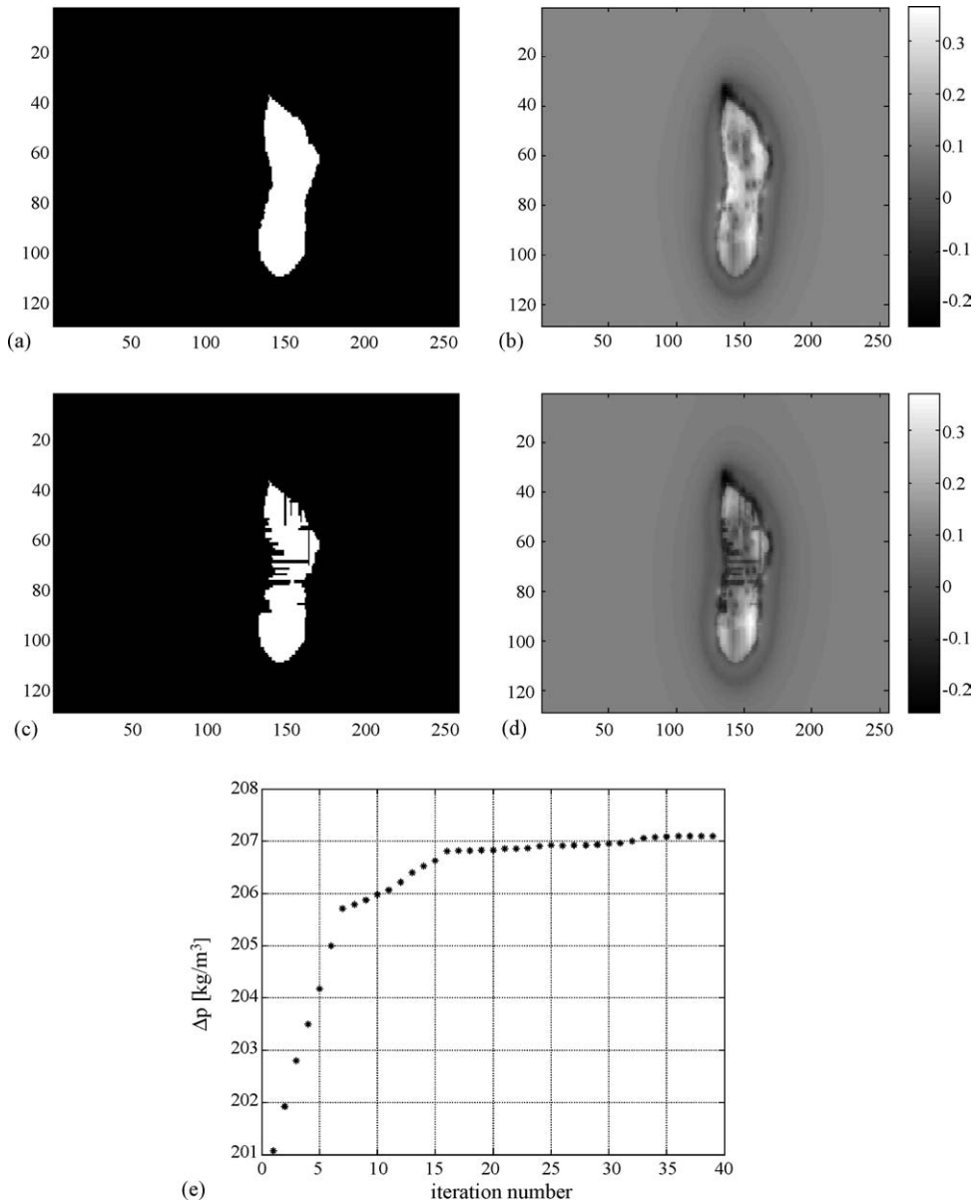

Fig. 8. Illustrating the inversion method. (a) The initial source model is the same as shown in Fig. 7b; (b) the difference between the unitless quantities $\Delta g/\Delta g_{\text{ext}}$ and $\Delta\rho/\Delta g_{\text{ext}}/\Delta\rho_{\text{unit}}/\Delta g_{\text{ext}}$ on, respectively, the left hand side and the right hand side of Eq. (2b) for the source model shown on (a); (c) the final source model after 39 iterations: (d) the same as (b), but for the source model shown on (c); (e) the value of $\Delta\rho$ changes throughout the iteration steps.

potential field modelling to be the same. Seismic profiles are expected to yield much more high frequency information along-profile than the results of gravimetric inversion.

The reliable part of the model is probably the estimated average mass density contrast $\Delta\rho$, because it requires the source model as a bulk to be located correctly. It should be noted that we have not used prior

information about the mass density (Goleby et al., 2000) to obtain this result. The mass density contrast was estimated simultaneously with the rough 3D source geometry. It is of course open for discussion whether the mass density estimation by Eq. (3), i.e. using only one extreme value, is adequate. To make it more robust, the mass density contrast could be estimated using more gravity points.

One final remark concerns our use of a very simple class of source models, equal-height-rectangular-homogeneous-vertical-prisms model. This choice is consistent with our philosophy of the robust and explicit assumptions. They were: (1) one source body generates each isolated anomaly; (2) the source body has a constant mass density contrast to the surroundings; (3) the horizontal extension of the source is reflected in the isolines of the surface gravity signal; (4) the misfit between the gravimetric response of the source model and the associated isolated gravity signal is mainly caused by the incorrect horizontal extension of the model.

The choice of the robust class of models has an advantage that such model cannot resolve all details of the surface gravity signal. In other words, the misfit function contains systematics caused by the choice of too rough class of models. One geological question, which is not clearly answered by the seismic profiles, is the direction of the tilt of the source body of the anomaly 1. Profile interpretations of Goleby et al. (2000) show for profile 2 a tilt to the east and on profile 5 a tilt to the south. These results were obtained mainly from detailed gravimetric data along the seismic profiles. Fig. 9 shows the residuals after 39 iteration steps (see Table 1). The unresolved parts of the gravity signal are along the eastern and the southern edge of the structure. Roughly, for the positive mass density contrast, it means that there should be more mass below these parts of the model than below other parts of the model. An east-south dipping structure with a positive mass density contrast would exactly have this effect. Thus, the interpretation of Goleby et al. (2000) on profiles was confirmed. Furthermore, our results seem to give a 3D systematics of this possible tilt, which only occurs locally in parts of the model.

Next would be to extend the class of source models to be flexible enough to include such tilts, e.g. by relaxing the imposed condition that the heights of all prisms should be the same. The advantage is, that this model should be a modification of the source models already obtained. If the modification is small

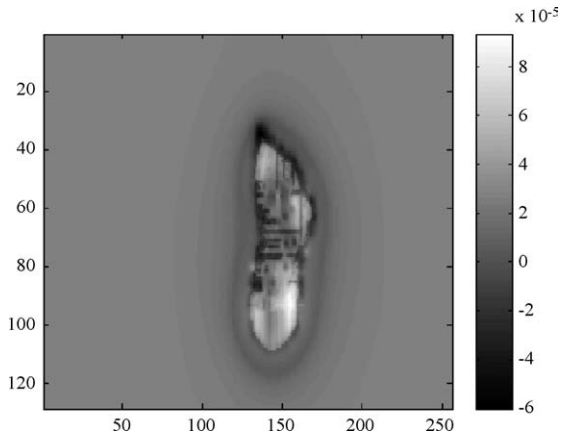

Fig. 9. Residual surface gravity signal (‘measured’ – ‘modelled’) for the gravity anomaly 1 (see Table 1). Unit: 10^{-5} m/s^2 (=mgal). Positive gravity residuals in the eastern and southern part of the model could indicate that the structure dips to SE. This is consistent with the profile interpretation (Goleby et al., 2000).

enough, the hope is that the model will yield robust results. The plausibility of such model is equivalent to the plausibility of the assumption of the dipping source.

4. Conclusions

In this paper we discuss a method of gravimetric inversion enhanced by the seismic information along profiles. A general multi-body inversion is transformed to a number of single-body inversions for a simple class of source models. For each single-body inversion problem the result is the construction of a rough 3D geometry of the source body and the estimation of its average mass density contrast to the surroundings. We emphasize the need of making conscious, explicit and geologically sound assumptions at every modelling step. The technique is illustrated by a complicated 3D multi-source modelling problem of the Yilgarn area in Western Australia. Based on seismic and gravimetric information along two profiles in the area we transform the general multi-source modelling problem into three single-body inversion problems. We estimate the average mass density contrast to the surroundings for these three source bodies, and determine the rough 3D source geometry for a simple model class; the source models are constructed from equal-height-rectangular-vertical-homogenous-prisms. The advantage of using such rough source models and the possible modifications of this model class are discussed. For the study area it is shown how the residuals of the misfit signal can be used to help solve open geological questions, the direction of the dip of the source body.

Acknowledgements

Australian Geodynamics Cooperative Research Centre (AGCRC) for alowing us to use the data. Dr. Fabio Boschetti visited Copenhagen on a travel grant founded by the Australian Research Council. Dr. Gábor Papp visited Copenhagen on a travel grant financed by the Danish Government Scholarschip under the Cultural Agreement between Denmark and Hungary. Dr. Peter Sorjonen-Ward, Finnish Geological Institute (formerly with CSIRO—Division of Exploration and Minning, Perth, Western Australia) for valuable discussions concerning the geological interpretation.

References

Boschetti, F., Therond, V., Hornby, P., 2004. Feature removal and isolation in potential field data. Geophys. J. Int. 159 (3), 833.

Goleby, B.R., Korsch, R.J., Sorjonen-Ward, P., Groenewald, P.B., Bell, B., Wyche, S., Bateman, R., Fomin, T., Drummond, B.J., Owen, A.J., 2000. Crustal Structure and Fluid Flow in the Eastern Goldfields, Western Australia: Results from the AGCRC's Yilgarn Deep Seismic Reflection Survey and Fluid Flow Modelling Projects. Australian Geological Survey Organisation, 100 pp.

Hornby, P., Boschetti, F., Horowitz, F.G., 1999. Analysis of potential field data in the wavelet domain. Geophys. J. Int. 137, 175–196.

Jackson, D.D., 1979. The use of a priori data to resolve non-unoqueness in linear inversion. Geophys. J. R. Astr. Soc. 57, 137–157.

Nagy, D., Papp, G., Benedek, J., 2000. The gravitational potential and its derivatives for the prism. J. Geodesy 74 (7/8), 552–560.

Poulet, T., D'Escrivan, H., Boschetti, F., Hornby, P., Horowitz, F., September 2001. New Advances In The Analysis of Potential Field Data By Multiscale Edges. ASEG, Brisbane.

Strykowski, G., 1996. Dealing with the non-uniqueness of the solution to the inverse geophysical problem. In: Hansen, C. (Ed.), Methodology and Application in Geophysics, Astronomy, Geodesy and Physics, Proceedings to the Interdisciplinary Inversion Workshop 4. Lyngby.

Strykowski, G., 1999. Some technical details concerning a new method of gravimetric-seismic inversion. Phys. Chem. Earth A 24, 207–214.

Strykowski, G., Boschetti, F., 2003. Discussion on "3-D inversion of gravity and magnetic data with depth resolution". Geophysics 68, 403–405 (Maurizio Fedi and Antonion Rapolla, Geophysics, 64, 452–461).

Wood, S.E. (Ed.), 1998. Extended Abstracts of AGCRC Workshop. Perth, 6 August 1998. Australian Geodynamics Cooperative Research Centre, Nedlands, 68 pp.